



# Graph theory network analysis provides brain MRI evidence of a partial continuum of neurodegeneration in patients with UMN-predominant ALS and ALS-FTD

Venkateswaran Rajagopalan<sup>a</sup>, Erik P. Pioro<sup>b,c,d,\*</sup>

<sup>a</sup> Department of Electrical and Electronics Engineering, Birla Institute of Technology and Science Pilani, Hyderabad Campus, Hyderabad 500078, India

<sup>b</sup> Neuromuscular Center, Department of Neurology, Neurological Institute, United States

<sup>c</sup> Department of Neurosciences, Lerner Research Institute, Cleveland Clinic, Cleveland, OH 44195, United States

<sup>d</sup> Neuromuscular Division, The Ken & Ruth Davee Department of Neurology, Northwestern University Feinberg School of Medicine, Chicago, IL 60611, United States

## ARTICLE INFO

### Keywords:

ALS  
ALS-FTD  
Brain network  
Grey matter  
White matter

## ABSTRACT

**Objective:** Our routine clinical neuroimaging showed hyperintense signal along the corticospinal tract only in some but not all patients with upper motor neuron (UMN)-predominant ALS. ALS patients with CST hyperintensity (ALS-CST+) and those without CST hyperintensity (ALS-CST-) present with nearly identical clinical UMN-predominant symptoms. Some previous studies have suggested that ALS patients with frontotemporal dementia (FTD) are on a continuum with ALS patients without FTD, while others have not.

We aimed to determine whether: (a) ALS-CST+, ALS-CST-, and ALS-FTD patients show differential sites of predominant neurodegeneration occurring primarily cortically in the perikaryon or subcortically in the white matter (WM), or (b) UMN-predominant ALS is on a continuum with ALS-FTD.

**Methods:** Exploratory whole brain grey matter (GM) voxel-based morphometry and WM network analysis using graph theory approach were performed. In this exploratory study, MRI data from 58 ALS patients (ALS-FTD,  $n = 15$ ; ALS-CST+,  $n = 19$ ; ALS-CST-,  $n = 24$ ) and 14 neurological controls were obtained.

**Results:** Significant differences in degree measures (evaluating WM networks) were observed between ALS patients and controls in frontal, motor, extra-motor, subcortical, and cerebellar regions. GM atrophy was observed only in the ALS-FTD subgroup and not in the other ALS subgroups.

**Conclusion:** Although WM network disruption by the ALS disease process showed different patterns between ALS-CST+, ALS-CST-, and ALS-FTD subgroups, there were some overlaps, particularly in prefrontal regions and between ALS-CST+ and ALS-FTD patients. Our preliminary findings suggest a partial continuum of, at least, WM degeneration between these subgroups with predominance of cortical pathology ("neuronopathy") in ALS-FTD patients and subcortical WM pathology ("axonopathy") in ALS-CST+ and ALS-CST- patients.

## 1. Introduction

Amiotrophic lateral sclerosis (ALS) is a fatal, progressive neurodegenerative disorder with unknown cause(s) (Mitsumoto et al., 1998). Since the discovery in 2006 that TDP-43 protein aggregation and mislocalization is a pathology common to ALS, frontotemporal lobar dementia, and ALS with frontotemporal dementia (ALS-FTD) (Neumann et al., 2006) these disorders have been proposed to be on a continuum. Neuroimaging and clinical studies provide evidence that ALS manifests with distinct clinical phenotypes identified by the extent of upper motor

neuron (UMN) dysfunction, lower motor neuron (LMN) dysfunction, and infrequently prominent cognitive impairment in patient with ALS and frontotemporal lobar dementia (ALS-FTD). A previous voxel based morphometry (VBM) study (Chang et al., 2005) revealed common patterns of grey matter (GM) atrophy in bilateral motor/premotor, frontal and temporal cortices of patients with either ALS or ALS-FTD suggesting that these two disorders are on a continuum. In keeping with this, another study (Lillo et al., 2012) using VBM analysis of GM and diffusion tensor imaging (DTI) of white matter (WM) with tensor based spatial statistics found overlapping abnormalities in anterior cingulate, motor

\* Corresponding author at: Neuromuscular Division, The Ken & Ruth Davee Department of Neurology, Northwestern University Feinberg School of Medicine, Chicago, IL 60611, United States.

E-mail address: [erik.pioro@northwestern.edu](mailto:erik.pioro@northwestern.edu) (E.P. Pioro).

<https://doi.org/10.1016/j.nicl.2022.103037>

Received 13 November 2021; Received in revised form 20 April 2022; Accepted 4 May 2022

Available online 8 May 2022

2213-1582/© 2022 The Authors. Published by Elsevier Inc. This is an open access article under the CC BY-NC-ND license (<http://creativecommons.org/licenses/by-nc-nd/4.0/>).

cortex and certain WM tracts of patients with ALS-FTD. In contrast to the above findings, a study (Omer et al., 2017) of FTD phenotypes (along the ALS-FTD spectrum) and of ALS patients without behavioral or cognitive deficits showed distinct patterns of GM and WM degeneration between these groups and across the FTD phenotypes suggesting that ALS and ALS-FTD are not on a continuum. This was further supported by recent findings of distinct cognitive and behavioral abnormalities in patients with UMN-predominant ALS as compared to those with behavioral FTD (Lulé et al., 2019).

Between 17% and 67% (median 40%) of ALS patients with predominantly UMN signs show bilateral corticospinal tract (CST) hyperintensities (ALS-CST+ patients) visible on conventional T2-, proton density-weighted, and FLAIR magnetic resonance imaging (MRI) (Mitsumoto et al., 1998). Interestingly, other ALS patients with similar UMN-predominant clinical features do not show such CST hyperintensity (ALS-CST- patients). On closer inspection, ALS-CST+ patients are significantly younger (Mitsumoto et al., 1998; Matte and Pioro, 2010), and have faster disease progression rate (DPR) with shorter survival times (Matte and Pioro, 2010) compared to ALS-CST- patients suggesting different disease mechanisms, although this is speculative. Assuming CST hyperintensities reflect degeneration of the UMN pathway (Abe et al., 1997), this can begin in the GM corticomotoneuron (as a neuronopathy) or in the subcortical WM (as an axonopathy). Therefore, the presence or absence of FTD or CST hyperintensities suggests that pathologic mechanisms vary between these ALS subgroups.

Differences of brain GM volume between controls and ALS patients without dementia have been found in some MRI studies (Sage et al., 2007); (Abrahams et al., 2005) but not in others (Chang et al., 2005); (Mezzapesa et al., 2007; Kassubek et al., 2005; Turner et al., 2007). DTI studies of WM using region of interest (ROI) localization showed reduced fractional anisotropy (FA) primarily in the posterior limb of the internal capsule (PLIC) in ALS patients compared to controls (Abe et al., 2004; Ellis et al., 1999; Graham et al., 2004; Jacob et al., 2003; Sach et al., 2004; Schimrigk et al., 2007). Using ROIs to select specific levels along the CST (Graham et al., 2004; Jacob et al., 2003; Sach et al., 2004; Schimrigk et al., 2007) limits identifying the tract's precise boundaries and measuring DTI changes along its entire rostrocaudal extent. For example, our earlier DTI study using an ROI approach, revealed no significant differences in FA values at four levels along the CST in ALS patients whether hyperintensity was present or not (Rajagopalan et al., 2013). However, our subsequent analysis using diffusion tensor tractography (DTT) showed significant reductions in CST fiber length and number between ALS-CST+ and ALS-CST- patients (Rajagopalan and Pioro, 2017). These results suggest that DTT is more likely to detect fiber abnormalities along the CST than are DTI metrics identified by ROIs at specific levels. Differential abnormalities in CST tracts of UMN-predominant ALS patients with or without CST hyperintensity, along with their contrasting demographics and rate of disease progression, support them as distinct ALS subtypes with possibly differing pathologies and even differing pathogenic mechanisms.

In this neuroimaging study, we aimed to understand whether: (a) ALS-CST+, ALS-CST-, and ALS-FTD are radiographically distinct phenotypes with differing locations of maximal neurodegeneration, and (b) whether these ALS subgroups are on a continuum. Based on our previous findings, we hypothesized that neurodegeneration in ALS-CST+ and ALS-CST- patients is primarily of subcortical WM (as an axonopathy), and in ALS-FTD patients is primarily of cortical GM perikarya (as a neuronopathy). Therefore, we hypothesized these ALS subgroups are not all on a continuum. To test these hypotheses, we performed 'exploratory' whole brain voxel-based morphometry (VBM) of GM and a graph theory-based whole brain WM network analysis. We chose graph theory network analysis because: (a) it uses the patient's own DTT-reconstructed virtual WM fiber tracts as compared to the more commonly employed ROI or tensor-based spatial statistics (TBSS) approaches; (b) its 'degree' measure reflects the importance of the node in a network; (c) it is a sensitive and common measure of centrality; and (d)

its physical interpretation is straightforward, e.g., a node with a high degree indicates it structurally (using DTI here) interacts with many other nodes (Rubinov and Sporns, 2010). If these hypotheses are correct, GM thickness/volume and whole brain WM networks would be differentially affected in ALS-CST+, ALS-CST-, and ALS-FTD patients.

## 2. Methods

### 2.1. Data acquisition

In accordance with the Declaration of Helsinki (1991), MRI and clinical data obtained as part of clinical neurological evaluation was approved by the Institutional Review Board at Cleveland Clinic to be stored and analyzed in de-identified fashion after patients provided verbal consent. Informed consent was obtained in accordance with the Declaration of Helsinki (1991) from the patient/kin. Detailed clinical evaluation (by EPP) included neurologic examination (motor and cognitive/behavioral assessment), electrodiagnostic testing, and brain MRI of neurologic controls and ALS patients enrolled into this study.

High resolution MPRAGE T1-, T2- and PD-weighted images and DTI data were obtained in 14 neurologic controls ( $n = 14$ , 9 males, 5 females) and 58 ALS patients who were clinically evaluated and diagnosed by EPP with the following clinicoradiologic phenotypes: (a) ALS-CST+ patients ( $n = 19$ , 14 males, 5 females) with predominantly UMN signs and CST hyperintensity visible on T2- and PD-weighted images; (b) ALS-CST- patients ( $n = 24$ , 13 males, 11 females) with predominantly UMN signs but no visible CST hyperintensity on MRI; and (c) ALS-FTD patients ( $n = 15$ , 4 males, 11 females) with classic ALS features of combined UMN and lower motor neuron (LMN) signs along with significant cognitive and/or behavioral impairment (supported by the Montreal Cognitive Assessment [MoCA] and formal neuropsychometric testing) and no visible CST hyperintensity.

UMN-predominant ALS patients at the time of MRI had prominent spasticity, hyperreflexia, and pathologic reflexes but little or no clinical or electrodiagnostic evidence of LMN signs; if present, the latter were restricted to mostly one neuraxial level (bulbar, cervical, or lumbosacral). On subsequent follow-up, all ALS-CST+ and ALS-CST- patients developed enough LMN abnormalities to meet El Escorial criteria of at least clinically probable ALS. UMN-predominant patients were included in the ALS-CST+ subgroup when CST hyperintensity was clearly visible on T2- plus PD-weighted images. This was noted most frequently at the cerebral peduncle and posterior limb of the internal capsule levels, with frequent identification along the corona radiata rostrally and even in WM subjacent to the precentral gyrus (primary motor cortex) (Matte and Pioro, 2010).

Clinical features of ALS patients are shown in Table 1. The demographic and clinical characteristics of neurological controls are given in Supplementary Table 1. Neurologic controls without UMN or obvious cognitive/behavioral impairment were chosen over healthy controls for a more stringent comparison to ALS patients.

The MoCA test (<https://www.mocatest.org>), where 26–30 is normal after adjustment for educational level, was the initial screening test used to identify cognitive dysfunction in study subjects. It confirmed cognitive impairment in ALS patients clinically suspected of having ALS-FTD with scores < 26 and usually < 20. Almost all cognitively impaired patients underwent formal neuropsychometric testing by a neuropsychologist, showing significant disturbances of behavior, cognition, executive function, and language (as shown in Supplementary Table 2). In addition, neurologic controls and UMN-predominant ALS patients included in this study displayed no clinical evidence of behavioral or cognitive impairment. MoCA testing of ALS patients in the latter group revealed scores within the normal range. Because all ALS patients were enrolled after routine clinical evaluation and those in the ALS-CST+ and ALS-CST- subgroups underwent only MoCA testing and not detailed cognitive/behavioral testing, more subtle abnormalities may have not been identified in these patients.

**Table 1**

Age, sample size and Clinical parameters of ALS patients.

Clinical measure of ALS subgroups	ALS-CST+	ALS-CST-	ALS-FTD	Statistical Significance
	Mean $\pm$ SD	Mean $\pm$ SD	Mean $\pm$ SD	
<i>n</i>	19	24	15	
Age (years)	50.7 $\pm$ 10.7	59.5 $\pm$ 12.1	66.2 $\pm$ 9.7	<i>P</i> = 0.0038
Symptom duration prior to MRI (months)	14.7 $\pm$ 7.8	48.4 $\pm$ 56.8	36.9 $\pm$ 21.7	<i>P</i> = 0.00045
ALSFRS-R score	34.0 $\pm$ 8.0	35.3 $\pm$ 6.8	29.2 $\pm$ 6.6	<i>P</i> = 0.045
DPR	1.45 $\pm$ 1.72	0.48 $\pm$ 0.45	1.28 $\pm$ 13.7	<i>P</i> = 0.0023
El Escorial Score	1.8 $\pm$ 1.01	1.34 $\pm$ 0.92	2.21 $\pm$ 1.25	<i>P</i> = 0.073

**Key:** ALS-CST+ - ALS patients with predominant upper motor neuron (UMN) signs and hyperintense signal along the corticospinal tract (CST) on conventional proton density- (PD) and T2-weighted images and no clinical dementia. ALS-CST- - ALS patients with predominant UMN signs without CST hyperintensity and no clinical dementia (ALS-CST-). ALSFRS-R - Revised ALS functional rating scale. DPR - Disease progression rate. SD - Standard deviation.

## 2.2. Imaging protocol

Imaging parameters were tailored for acquisition during routine clinical imaging on a 1.5 T Siemens Symphony scanner (Erlangen, Germany) of patients being evaluated for ALS. Clinical T2- and PD-weighted images were obtained to assess CST hyperintensity using dual-echo fast spin echo sequences whose imaging parameters included: slice thickness = 4 mm, in-plane resolution =  $0.9 \times 0.9$  mm; TR = 3900 ms, TEs = 26 ms (for PD) and 104 ms (for T2), total scan time = 3.5 min. DTI data were acquired during routine clinical scanning, which because of time constraints resulted in some compromises although still providing adequate quality data for quantitative analyses. Single shot-echo planar imaging (SS-EPI) sequence was used to acquire 12 diffusion-weighted ( $b = 1000$  s/mm<sup>2</sup>) images and one  $b = 0$  s/mm<sup>2</sup> image. Imaging parameters included: resolution  $1.9 \times 1.9 \times 4$  mm<sup>3</sup>, repetition time TR = 6000 ms, echo time TE = 121 ms, EPI factor = 128, and scan time = 7.5 min. T1-weighted data were obtained using 3D magnetization-prepared rapid gradient echo (M-PRAGE) sequence. Imaging parameters included: 160 slices, voxel resolution of  $1.0 \times 1.0 \times 1.0$  mm, TR = 1970 ms, TE = 4.38 ms, and scan time = 6.5 min.

## 3. Data processing

### 3.1. Grey matter VBM analysis

Grey matter VBM analysis was carried out in SPM8 software (<https://www.fil.ion.ucl.ac.uk/spm/>) (Ashburner, 2009) using VBM8 toolbox. We have adopted standard VBM processing routines which included: (a) estimate and write, (b) DARTEL create template, (c) DARTEL existing template, (d) normalize to MNI space, and (e) parametric statistical inference. Briefly, the first step (estimate and write) involved bias-correcting the raw T1-weighted images for inhomogeneities, extracting the brain, and segmenting it into GM, WM and CSF volume probability maps. The DARTEL create template step generated a customized template to which all subjects were nonlinearly registered using the existing DARTEL template module. The resulting images were modulated, smoothed using a 7 mm full-width half-maximum (FWHM), and used for statistical inference. Age was added as a covariate and regressed out; this was not done for gender as our previous studies (Rajagopalan and Pioro, 2014) (as shown in Supplementary Fig. 1) revealed no effect. *P* < 0.05 corrected for multiple comparisons using family-wise error rate was considered the level of

significance. Voxel-wise inference in GM volumes between the ALS patient subgroups and controls was considered.

### 3.2. DTI data pre-processing

DTI data preprocessing using openware ExploreDTI (<http://www.exploredti.com/>) (Leemans et al., 2009) included: (a) eddy current and motion correction, (b) fitting of corrected images using robust diffusion tensor estimation approach, (c) performing whole brain tractography using deterministic streamline approach with fractional anisotropy (FA) thresholds of starting = 0.2 and stopping = 1, (d) registering all ROIs from this atlas template to each of the subject's space, and (e) obtaining connectivity matrices using 116 ROIs from the Automated Anatomical Labeling (AAL) atlas (Tzourio-Mazoyer et al., 2002). The adjacency matrix across all these ROIs for each subject was obtained for DTI metrics FA, axial diffusivity (AD), reflecting axonal integrity and a potential marker of wallerian degeneration, and radial diffusivity (RD), reflecting myelin integrity. Previous ALS studies (Dimond et al., 2017; Tang et al., 2015), including one using WM network analysis (Dimond et al., 2017) reported FA to be a sensitive DTI measure in detecting WM degeneration in ALS and indicated the reliability of FA measures in diagnosing ALS. Even though FA is sensitive, it is not specific to microstructural changes as are AD and RD (Alexander et al., 2007). In addition to measuring FA, therefore, it is recommended (Alexander et al., 2007) to assess AD, RD or mean diffusivity (MD). Since our primary focus was to determine the axonal and myelin degeneration in ALS, we included AD and RD networks but not MD as it reflects changes of edema, inflammation and necrosis (Alexander et al., 2007).

### 3.3. Graph theory network analysis

Graph analysis toolbox (GAT) software (<https://www.nitrc.org/projects/gat/>) (Hosseini et al., 2012) was used to perform whole brain WM network analysis. The connectivity matrix obtained using ExploreDTI (see above) was imported into GAT software for further processing. The connectivity strength between nodes was calculated using FA-, AD- and RD- weighted streamlines. Using GAT diffusion toolbox, individual network measures were derived with the "network measures" module. From these, we considered only the 'degree' measure in an effort to not over-complicate analyses in this exploratory study. At this time, we did not analyze other graph theory parameters, including path length (more suitable with measures like 'small worldness') and centrality.

Networks of controls and patient groups were compared over the range of densities from 0.04 to 0.14 with interval steps of 0.01 and the minimum network density threshold of 0.05.

Age was added as a covariate and regressed out. Since gender did not show any significant effect in our previous WM studies (Rajagopalan et al., 2013; Rajagopalan et al., 2013), it was not regressed out. Statistical comparisons for between group differences were tested using non-parametric permutation approach with 1000 repetitions. Two-sample *t*-test was used to compare subgroups of control vs ALS-FTD, control vs ALS-CST+, and control vs ALS-CST- with a significance value of *P* < 0.05. Multiple comparison correction across the 116 ROI brain nodes was performed using false discovery rate (FDR). Unfortunately, the GAT toolbox unlike SPM's GLM model does not have a statistics plugin to compare more than two groups at once. Since our preliminary study is 'exploratory' with a small imaging data set, we elected to correct for multiple comparisons as done in SPM's GLM model rather than by the more stringent Bonferroni method. Because no statistical comparison was performed among the ALS patient groups, we did not regress out the effect of clinical measures, namely: duration of symptoms prior to MRI, ALSFRS-R score, El Escorial Criteria score, and DPR.

### 3.4. Clinical measures

Duration of symptoms prior to MRI, ALSFRS-R score, El Escorial

Criteria (Brooks et al., 2000) and DPR were obtained from ALS patients (calculated using the expression below). For the purpose of this study, we have converted the descriptive terms used in the El Escorial criteria describing the extent of UMN and LMN dysfunction along the body's neuraxial levels in increasing extent as: Possible ALS, Probable with Laboratory Support ALS, Probable ALS, and Definite ALS, to numerical values of 1, 2, 3, and 4, respectively. Correlations between graph metrics and the above clinical measures were performed using Spearman's correlation coefficient after correcting for multiple comparisons using FDR for the ROIs and using the Bonferroni method for the three ALS subgroups with  $P < 0.017$ . Also, clinical measures were correlated with GM volume changes in VBM with  $P < 0.05$ .

$$\text{DPR(Disease Progression Rate)} = \frac{(48 - \text{ALSFRS} - \text{R at MRI})}{\text{Duration of symptoms (mos)}}$$

#### 4. Results

GM volume was significantly reduced in frontal, temporal, and cerebellar regions only in the ALS-FTD group when compared to controls ( $P < 0.05$ ) as listed in Table 2 and shown in Fig. 1. However, no significant differences in GM volume were seen in the other ALS subgroups (ALS-CST+, ALS-CST-) when compared to controls. No significant correlations were observed between the clinical measures and GM volumes.

Region-wise comparison of graph theory metric degree across the 116 AAL atlas brain nodes of networks using DTI metrics FA, AD and RD between controls and the three patient subgroups revealed multiple regions of abnormality in the ALS patients. The 88 areas where node degree measures/values were significantly ( $P < 0.05$ ) different between patient subgroups and controls are detailed in Table 3 listing cortical, subcortical and cerebellar regions. Between ALS patient subgroups, differences of regional WM involvement were limited, although some similarities and overlaps were noted. Color-coding in Table 3 indicates regions where abnormalities overlapped between the three ALS subgroups. The greatest number of significant similarities was detected in several forebrain areas between ALS-CST+ and ALS-FTD subgroups. Overlap was also found in several cerebellar regions between ALS-CST+ and ALS-CST- subgroups (see Table 3). Figs. 2–4 show the distributions of these WM abnormalities on brain projections in each subgroup individually and in combination with each other. Fig. 5 represents the extent of overlap between the ALS subgroups in a Venn diagram format; percentages of overlap are calculated based on the total number ( $n = 88$ ) of statistically significant areas identified.

Symptom duration was shorter ( $P = 0.01$ ) and DPR was faster ( $P = 0.01$ ) in the ALS-CST+ subgroup compared to the ALS-CST- subgroup at the time of MRI. No significant correlations were observed between the degree values of node regions and clinical measures after correcting for multiple comparisons using FDR except for RD-derived degree values in

two patient subgroups. DPR strongly correlated with RD-derived degree values in ALS-FTD patients in the right hippocampus ( $r = 0.83$ ,  $P = 0.0112$ ) and right angular gyrus ( $r = -0.83$ ,  $P = 0.0112$ ). In addition, RD-derived degree values in ALS-CST+ patients strongly correlated with the ALSFRS-R score in the right superior frontal gyrus, orbital part ( $r = -0.71$ ,  $P = 0.0172$ ) and right superior frontal gyrus, medial orbital ( $r = -0.75$ ,  $P = 0.0103$ ).

#### 5. Discussion

Significant GM volume differences were observed only between controls and ALS-FTD patients, indicating the inherent difference in the distribution of pathology between ALS patients with clinically detected cognitive dysfunction or dementia and those without. Non-motor frontal and prefrontal areas are responsible for executive functions, behavioral and emotional regulation. Other extra-motor regions affected include temporal gyrus (cognitive functions) and cerebellum, supporting the view of ALS-FTD as a multisystem disorder (Strong, 2001). Other studies (Sage et al., 2007); (Abrahams et al., 2005) have also not found significant GM volume differences between controls and non-demented ALS patients.

Degree of the WM network using FA measure in patients with ALS-FTD affects the frontal lobe, temporal lobe, precentral gyrus, hippocampus, cingulum, and occipital regions. In these ALS-FTD patients, our GM and WM results revealed greater frontal than temporal lobe degeneration, with many frontal lobe regions showing significant differences. While only frontal and cerebellar regions were involved in the ALS-CST- subgroup, the ALS-CST+ subgroup revealed significant degree changes in frontal, temporal, parietal and cerebellar regions. Of note, lack of overlapping FA network changes between ALS-CST+, ALS-CST- and ALS-FTD subgroups supports the view that UMN-predominant ALS and ALS-FTD are not on a full continuum. Similar to the above FA results, AD degree values were significantly different between ALS-FTD patients and controls predominantly in WM networks underlying several frontal regions, including the cingulum. WM FA networks were affected in ALS-CST+ patients underlying frontal, cingulum, occipital and cerebellar regions, and in ALS-CST- patients underlying frontal and cerebellar regions. Although FA networks showed no overlap of affected brain nodes between ALS-CST+, ALS-CST- and ALS-FTD patients, RD-based WM networks did. Brain regions in all three subgroups where only RD networks were abnormal (suggesting damage to myelin), included: inferior frontal gyrus (orbital part), angular gyrus, and olfactory cortex. Based on RD (but not FA or AD) network changes, these frontal lobe region nodes primarily on the right comprise a limited but important core of WM pathology common to ALS-CST+, ALS-CST- and ALS-FTD patients.

In addition to abnormalities in motor regions, significant WM network damage in all three ALS patient subgroups was found in common prefrontal areas, which are related to language and cognitive or behavioral functions. Such consistent pathology in premotor regions of ALS-CST+, ALS-CST- and ALS-FTD patients has not been reported previously and warrants further study. Its relevance is unclear since only ALS-FTD patients had clinically detectable cognitive and behavioral abnormalities, including language dysfunction. Such white matter changes in the non ALS-FTD groups may indicate an earlier stage of degeneration prior to clinical deficit, considering GM overlying these regions was affected only in the ALS-FTD subgroup. Although patients in ALS-CST+ and ALS-CST- subgroups underwent only routine MoCA neuropsychometric evaluation, they showed no clinical evidence of cognitive or behavioral dysfunction in accordance with the Neary et al. (1998) and Rascovsky et al. (2011) criteria. Nonetheless, because ALS-CST+ and ALS-CST- patients did not undergo detailed neurocognitive testing, subtle cognitive abnormalities may not have been identified. If this were the case, however, more overlapping regions should be observed with both of these ALS subgroups and the ALS-FTD patients rather than with only ALS-CST+ patients.

**Table 2**  
Brain regions showing significant GM atrophy in ALS-FTD patients compared to neurologic controls.

MNI coordinates	Region Name
-10 18 -23	Frontal_Sup_Orb_L
-6 26 -21	Rectus_L
38 21 -12	Frontal_Inf_Orb_R
32 20 -18	Insula_R
-14 27 55	Frontal_Sup_L
-30 15 -21	Frontal_Inf_Orb_L
-32 15 -3	Insula_L
14 48 42	Frontal_Sup_R
64 -33 28	Supramarginal_R
54 15 4	Frontal_Inf_Oper_R
14 15 -12	Rectus_R
-39 -30 -29	Cerebellum_6_L
32 17 52	Frontal_Mid_R
12 11 -6	Caudate_R
64 -37 1	Temporal_Mid_R

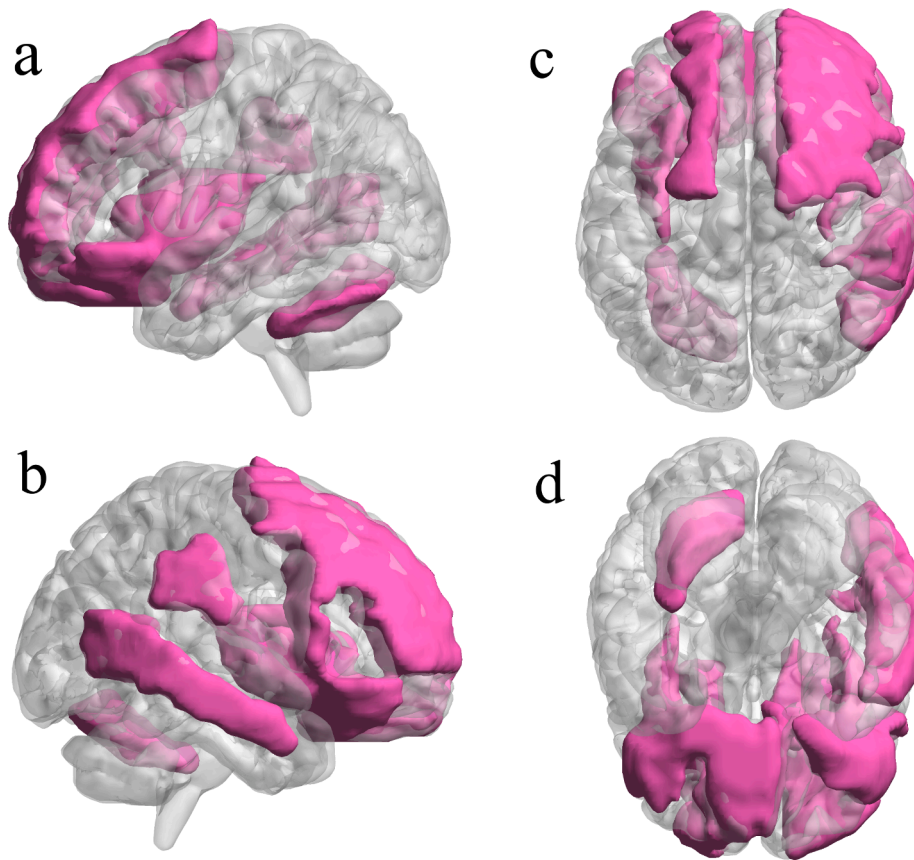


**Fig. 1.** Brain regions with significant differences in grey matter VBM between patients with ALS-FTD and neurologic controls in (a) lateral left hemisphere, (b) lateral right hemisphere, (c) superior and (d) inferior views.

A previous connectomics study (Verstraete et al., 2011) reported abnormalities in the precentral gyrus, pallidum, hippocampus, caudal middle frontal gyrus, posterior cingulate and precuneus of patients with ALS. Reductions of degree measure in regions outside the precentral gyrus i.e. postcentral gyrus, caudate, insula, amygdala, cuneus, and temporal pole suggest extramotor involvement in such patients. These results are consistent with the view that ALS is a multisystem disorder extending beyond the motor system (Rajagopalan and Pioro, 2014; Verstraete et al., 2011; Filippini et al., 2010). Our results concur with findings of Verstraete et al (Verstraete et al., 2011) that neurodegeneration in ALS affects not only the primary motor WM network but also its connections to supplemental motor, precuneus and posterior cingulate regions.

Correlation analyses between clinical and neuroimaging metrics revealed strong relationships between DPR and node degree of ALS-FTD patients in the right angular gyrus and right hippocampus. Correlations were negative in the right angular gyrus and positive in the right hippocampus, indicating that faster disease progression is associated with weaker or fewer connections (node degree) with the angular gyrus and stronger or more connections with the hippocampus. The significance of these changes in the latter region is unclear at present but may be compensatory (to retain stable brain function) by establishing more connections between the right hippocampus and other brain regions. In contrast, ALS-CST+ patients showed strong positive correlations with lower degree values in right superior frontal gyrus (orbital and medial orbital parts) and lower (worsening) ALSFRS-R scores.

Three striking findings of our present study include the: (a) minimal overlap in brain regions revealing significant GM and WM damage between controls and all three ALS subgroups, (b) more frequent overlap of WM abnormalities between ALS-FTD and ALS-CST+ than with ALS-CST- patients, and (c) higher number of cerebellar regions with WM

changes in ALS-CST+ and especially ALS-CST- subgroups compared to the ALS-FTD subgroup (see Figs. 2-4, Table 3). This suggests only limited degree of overlap and continuity between these three ALS subgroups, occurring primarily in olfactory, inferior frontal (orbital), and angular gyrus regions (see Fig. 4, Table 3).

Our previous analysis of the CST showed WM damage (represented by changes in FA, AD, RD, and mean diffusivity) in these ALS subgroups (Rajagopalan et al., 2013). Our earlier DTT study (Rajagopalan and Pioro, 2017) demonstrated “truncation” of CST WM fibers predominantly in ALS-CST+ patients compared to ALS-CST- patients. The graph theory results here provide additional evidence that pathophysiologic changes in ALS differ between UMN-predominant ALS patients with and without CST hyperintensity. Only WM connections underlying the superior frontal gyrus and in cerebellar lobules VIII, IX, and X show overlapping degeneration in ALS-CST+ and ALS-CST- subgroups. Interestingly, ALS-CST+ patients share several brain areas of WM degeneration with ALS-FTD patients. These findings suggest that the two latter ALS phenotypes share common pathogenic mechanisms that are not shared with the ALS-CST- phenotype.

The significant GM degeneration in ALS-FTD patients was not observed in the other two patient subgroups and suggests a predominant neuronopathy. Furthermore, the more prominent WM degeneration in ALS-CST+ and ALS-CST- patients compared to those with ALS-FTD suggests a predominant ‘axonopathy’. Taken together, therefore, the GM VBM and brain WM network results suggest a GM to WM continuum between ALS-FTD and UMN-predominant ALS (represented by ALS-CST+ and ALS-CST- patients). Despite differences of WM abnormality in brain areas of ALS-CST+, ALS-CST- and ALS-FTD phenotypes, regions of overlap indicate a partial continuum of the disease process.

**Table 3**

Brain regions showing overlap and no-overlap of WM abnormalities between ALS patient subgroups.

ALS Subgroup	ALS-CST+			ALS-CST-			ALS-FTD		
	FA	AD	RD	FA	AD	RD	FA	AD	RD
<b>Brain Region - Cortical</b>									
Sup. Frontal gy. (dorsolateral)-L	Y	Y	Y	Y	Y	Y			
Sup. Frontal gy. (dorsolateral)-R	Y	Y	Y						
Sup. Frontal gy. (med. orbital)-L			Y	Y			Y	Y	Y
Sup. Frontal gy. (med. orbital)-R			Y	Y			Y	Y	Y
Sup. Frontal gy. (orbital pt.)-L			Y	Y			Y	Y	Y
Sup. Frontal gy. (orbital pt.)-R			Y	Y			Y	Y	Y
Sup. Frontal gy. (medial)-L		Y	Y						
Sup. Frontal gy. (medial)-R		Y	Y	Y					
Mid. Frontal gy.-L		Y	Y						
Mid. Frontal gy.-R		Y	Y						
Mid. Frontal gy. (orbital pt.)-L		Y	Y				Y	Y	Y
Mid. Frontal gy. (orbital pt.)-R							Y	Y	Y
Inf. Frontal gy. (orbital pt.)-L		Y	Y			Y	Y	Y	Y
Inf. Frontal gy. (orbital pt.)-R		Y	Y			Y	Y	Y	Y
Inf. Frontal gy. (opercular pt.)-L				Y					
Inf. Frontal gy. (opercular pt.)-R				Y	Y				
Inf. Frontal gy. (triangular pt.)-L						Y			
Inf. Frontal gy. (triangular pt.)-R				Y	Y	Y			
Precentral gy.-L							Y		Y
Precentral gy.-R									
Postcentral gy.-L									Y
Postcentral gy.-R									Y
Gyrus rectus-L							Y		Y
Gyrus rectus-R									
Olfactory cortex-L				Y	Y		Y	Y	Y
Olfactory cortex-R			Y	Y	Y		Y	Y	Y
Ant. Cingulate gy.-L		Y	Y				Y	Y	Y
Ant. Cingulate gy.-R		Y	Y				Y	Y	Y
Post. Cingulate gy.-L		Y						Y	
Post. Cingulate gy.-R									
Paracingulate gy.-L		Y	Y				Y	Y	Y
Paracingulate gy.-R		Y	Y				Y	Y	Y
Insula-L									
Insula-R							Y	Y	Y
Angular gy.-L									
Angular gy.-R		Y	Y	Y			Y	Y	Y
Supramarginal gy.-L									
Supramarginal gy.-R									
Parahippocampal gy.-L									
Parahippocampal gy.-R			Y						
Mid. Temporal gy.-L									Y
Mid. Temporal gy.-R									
Sup. Temporal gy.-L						Y			
Sup. Temporal gy.-R									
Sup. Temporal gy. (temp. pole)-L	Y	Y					Y	Y	
Sup. Temporal gy. (temp. pole)-R									
Paracentral lobule-L	Y	Y							
Paracentral lobule-R									
Sup. Parietal-L									
Sup. Parietal-R	Y								
Inf. Parietal-L			Y						
Inf. Parietal-R	Y	Y							
Cuneus-L									
Cuneus-R							Y		
Precuneus-L									Y
Precuneus-R		Y					Y	Y	Y
Sup. Occipital gy.-L							Y	Y	Y
Sup. Occipital gy.-R									
Mid. Occipital gy.-L		Y							
Mid. Occipital gy.-R		Y							
Inf. Occipital gy.-L				Y			Y	Y	Y
Inf. Occipital gy.-R									
Calcarine Cx-L									
Calcarine Cx-R			Y						

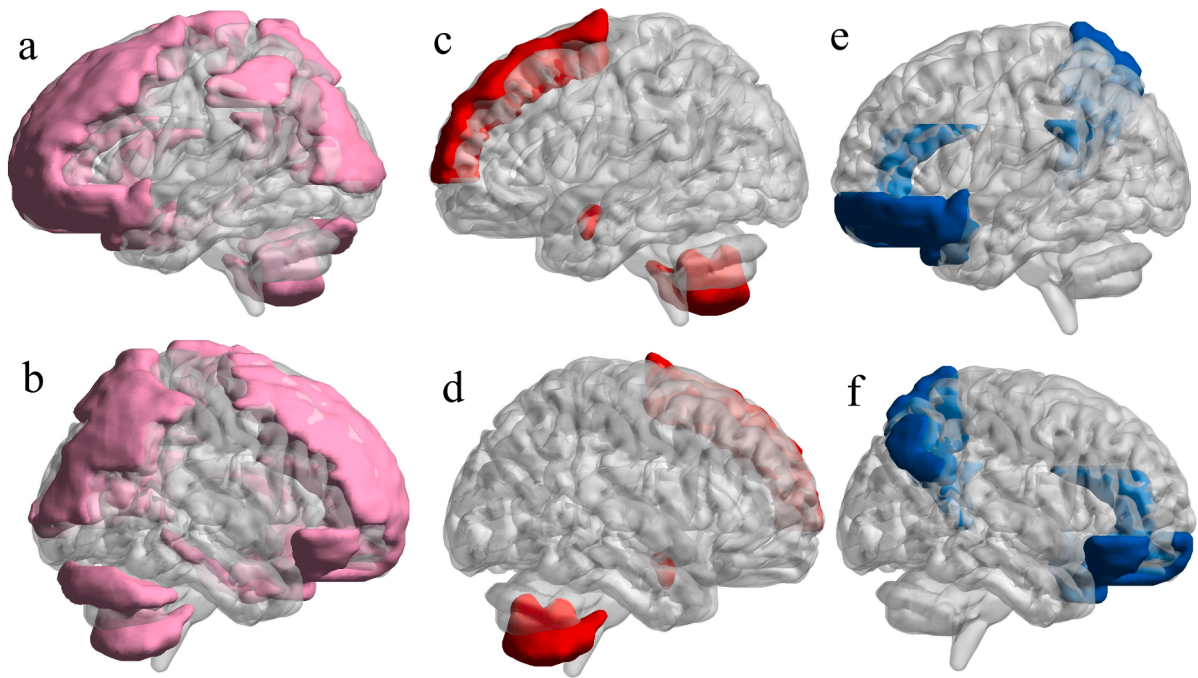
  

ALS Subgroup	ALS-CST+			ALS-CST-			ALS-FTD		
	FA	AD	RD	FA	AD	RD	FA	AD	RD
<b>Brain Region- Subcortical &amp; Cerebellar</b>									
Thalamus-L								Y	Y
Thalamus-R									
Caudate-L		Y	Y	Y					
Caudate-R									
Hippocampus-L									
Hippocampus-R								Y	Y
Amygdala-L					Y		Y	Y	
Amygdala-R									Y
Cerebellum IV-L								Y	Y
Cerebellum IV-R								Y	Y
Cerebellum V-L								Y	Y
Cerebellum V-R									
Cerebellum VI-L					Y	Y			
Cerebellum VI-R									
Cerebellum VIII-L									
Cerebellum VIII-R		Y	Y		Y	Y	Y		
Cerebellum IX-L					Y	Y	Y		
Cerebellum IX-R					Y	Y	Y		
Cerebellum X-L					Y	Y	Y	Y	Y
Cerebellum X-R		Y	Y	Y	Y	Y	Y	Y	Y
Cerebellum crus I-L									
Cerebellum crus I-R		Y	Y					Y	
Cerebellum crus II-L									
Cerebellum crus II-R					Y	Y			

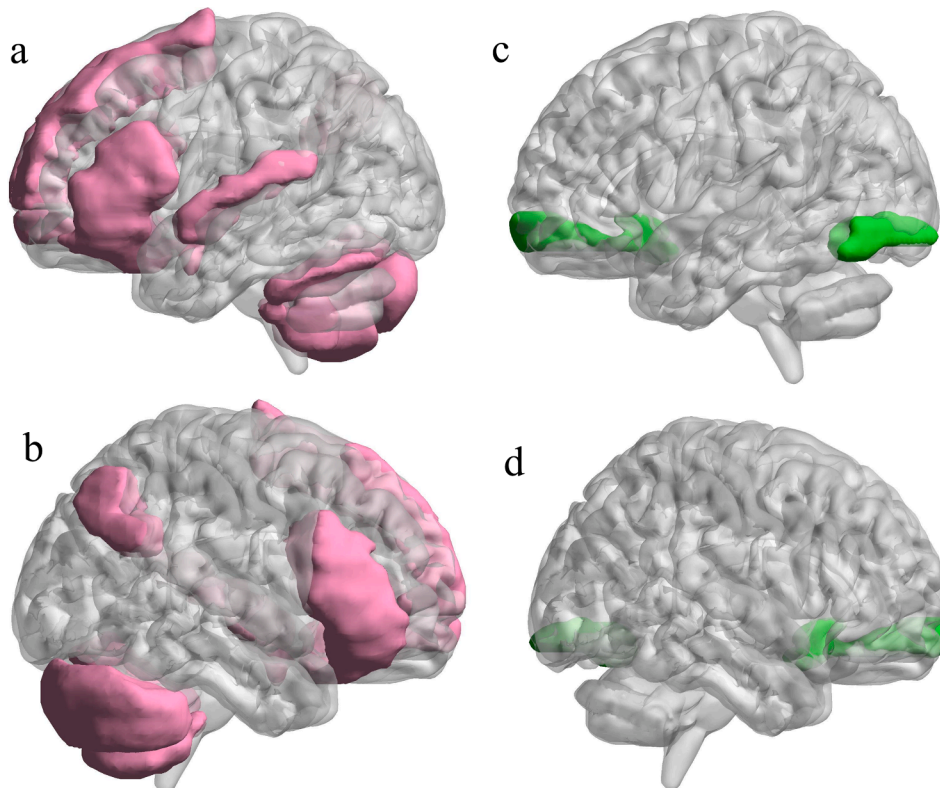
  

**KEY - Abnormalities shared by:**

- ALS-CST+ & ALS-CST- ■
- ALS-CST+ & ALS-FTD ■
- ALS-CST- & ALS-FTD ■
- All three ■



**Fig. 2.** Brain regions with significant WM degeneration shown by FA-, AD- and RD- weighted networks in left (a, c, e) and right (b, d, f) hemispheres of ALS-CST+ patients alone (pink, a, b), and overlapping with ALS-CST- patients (red, c, d), and ALS-FTD patients (blue, e, f). (See [Table 3](#) for details of overlapping areas of abnormality between subgroups indicated by red and blue colors.)



**Fig. 3.** Brain regions with significant WM degeneration shown by FA-, AD- and RD- weighted networks in left (a, c) and right (b, d) hemispheres of ALS-CST- patients alone (pink, a, b), and overlapping with ALS-FTD patients (green, c, d). (See [Table 3](#) for details of overlapping areas of abnormality between subgroups indicated by green color.)

## 6. Conclusion

Although differences in whole brain GM atrophy and WM networks

between ALS-CST+, ALS-CST-, and ALS-FTD groups exist, the minimal overlap identified suggests that these ALS subgroups are on a partial continuum. The closer similarity of WM degeneration between ALS-

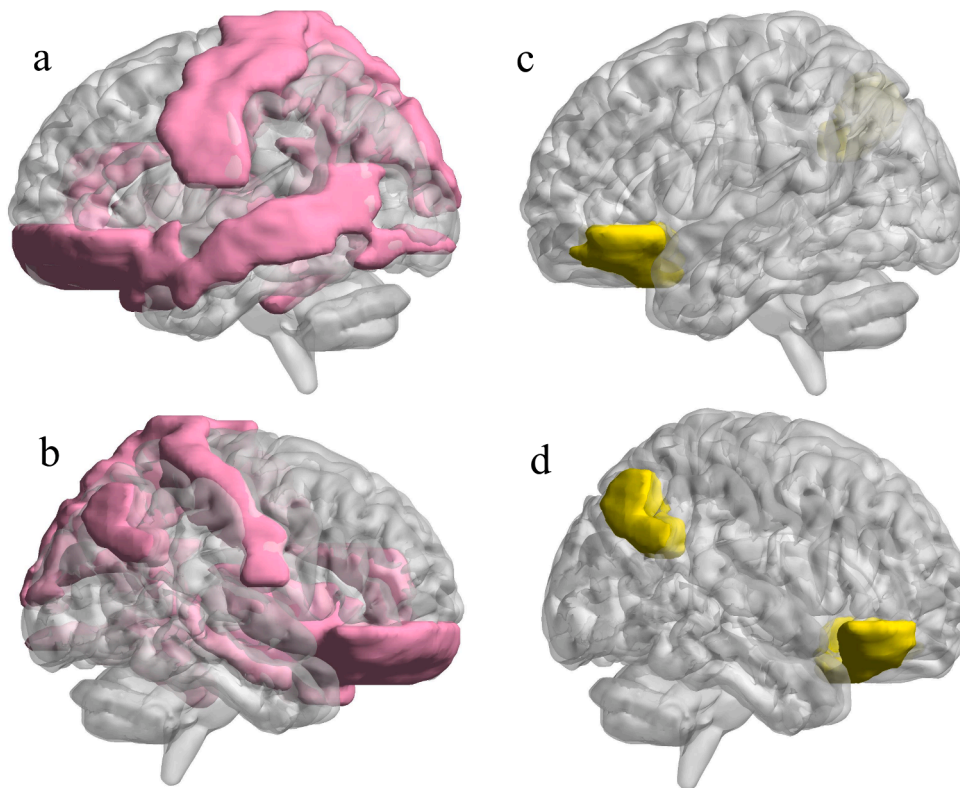


**Fig. 4.** Brain regions with significant WM degeneration shown by FA-, AD- and RD- weighted networks in left (a, c) and right (b, d) hemispheres of ALS-FTD patients alone (pink, a, b), and overlapping with ALS-CST+ and ALS-CST- patients (yellow, c, d). (See Table 3 for details of overlapping areas of abnormality between subgroups indicated by yellow color.)

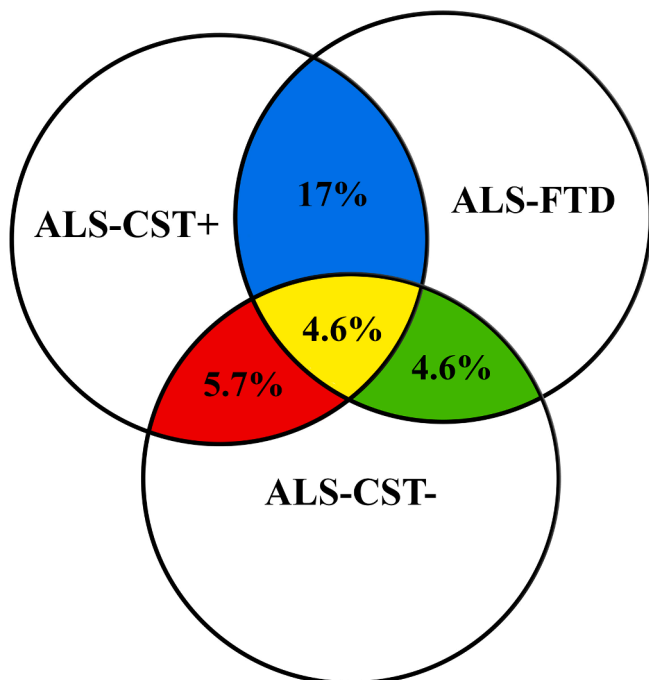


**Fig. 5.** Venn diagram representing estimated overlap of WM abnormalities (with percentages) in brain regions of the three ALS patient subgroups, as revealed by graph theory analysis. Extent of abnormalities shared by ALS-CST+ and ALS-CST- patients = red, by ALS-CST+ and ALS-FTD patients = blue, by ALS-CST- and ALS-FTD patients = green, and by all three subgroups = yellow. (See Table 3 for details of overlapping areas of abnormality between subgroups indicated by red, blue, green and yellow colors.)

CST+ and ALS-FTD patients than between ALS-CST+ and ALS-CST- patients is of particular interest. Significant correlations between node degree and clinical measures indicate that graph metric degree can provide neuroimaging-based biomarkers for at least ALS-CST+ and ALS-FTD subgroups. Future studies with histopathological data from ALS-CST+, ALS-CST- and ALS-FTD subgroups may provide further insights into our findings.

**Conflict of Interest.**

The authors report no conflict of interest related to the topic of this manuscript. EPP has received clinical trial and/or research funding from the ALS Association, Biogen, Inc., Biohaven Pharmaceuticals, NIH/CDC, and the Samuel J. and Connie M. Frankino Charitable Foundation. He has received consulting fees from Argenx, Avanir Pharmaceuticals, Inc., Biohaven Pharmaceuticals, Inc., Cytokinetics, Inc., ITF Pharma, Inc., MT Pharma America, Inc., Neurotherapia, Inc., and Otsuka America, Inc.

**7. Data sharing**

The data used in this study are property of Cleveland Clinic and therefore, cannot be shared.

**Declaration of Competing Interest**

The authors declare that they have no known competing financial interests or personal relationships that could have appeared to influence the work reported in this paper.

**Acknowledgements**

The authors thank all the patients who participated in this study.

## Funding

We did not receive any funding support for this study.

## Appendix A. Supplementary data

Supplementary data to this article can be found online at <https://doi.org/10.1016/j.nicl.2022.103037>.

## References

- Abe, K., Fujimura, H., Kobayashi, Y., Fujita, N., Yanagihara, T., 1997. Degeneration of the pyramidal tracts in patients with amyotrophic lateral sclerosis. A premortem and postmortem magnetic resonance imaging study. *J. Neuroimaging* 7 (4), 208–212.
- Abe, O., Yamada, H., Masutani, Y., Aoki, S., Kunimatsu, A., Yamasue, H., Fukuda, R., Kasai, K., Hayashi, N., Masumoto, T., Mori, H., Soma, T., Ohtomo, K., 2004. Amyotrophic lateral sclerosis: diffusion tensor tractography and voxel-based analysis. *NMR Biomed.* 17 (6), 411–416.
- Abrahams, S., Goldstein, L.H., Suckling, J., Ng, V., Simmons, A., Chitnis, X., Atkins, L., Williams, S.C.R., Leigh, P.N., 2005. Frontotemporal white matter changes in amyotrophic lateral sclerosis. *J. Neurol.* 252 (3), 321–331.
- Alexander, A.L., Lee, J.E., Lazar, M., Field, A.S., 2007. Diffusion tensor imaging of the brain. *Neurotherapeutics* 4 (3), 316–329.
- Ashburner, J., 2009. Computational anatomy with the SPM software. *Magn. Reson. Imaging* 27 (8), 1163–1174.
- Brooks, B.R., Miller, R.G., Swash, M., Munsat, T.L., 2000. El Escorial revisited: revised criteria for the diagnosis of amyotrophic lateral sclerosis. *Amyotroph. Lateral Scler. Other Motor Neuron Disord.* 1 (5), 293–299.
- Chang, J.L., Lomen-Hoerth, C., Murphy, J., Henry, R.G., Kramer, J.H., Miller, B.L., Gorno-Tempini, M.L., 2005. A voxel-based morphometry study of patterns of brain atrophy in ALS and ALS/FTLD. *Neurology*. 65 (1), 75–80.
- Dimond, D., Ishaque, A., Chenji, S., Mah, D., Chen, Z., Seres, P., Beaulieu, C., Kalra, S., 2017. White matter structural network abnormalities underlie executive dysfunction in amyotrophic lateral sclerosis. *Hum. Brain Mapp.* 38 (3), 1249–1268.
- Ellis, C.M., Simmons, A., Jones, D.K., Bland, J., Dawson, J.M., Horsfield, M.A., Williams, S.C.R., Leigh, P.N., 1999. Diffusion tensor MRI assesses corticospinal tract damage in ALS. *Neurology*. 53 (5), 1051.
- Filippini, N., Douaud, G., Mackay, C.E., Knight, S., Talbot, K., Turner, M.R., 2010. Corpus callosum involvement is a consistent feature of amyotrophic lateral sclerosis. *Neurology*. 75 (18), 1645–1652.
- Graham, J.M., Papadakis, N., Evans, J., Widjaja, E., Romanowski, C.A.J., Paley, M.N.J., Wallis, L.L., Wilkinson, I.D., Shaw, P.J., Griffiths, P.D., 2004. Diffusion tensor imaging for the assessment of upper motor neuron integrity in ALS. *Neurology*. 63 (11), 2111–2119.
- Hosseini, S.M.H., Hoefft, F., Kesler, S.R., Lambiotte, R., 2012. GAT: a graph-theoretical analysis toolbox for analyzing between-group differences in large-scale structural and functional brain networks. *PLoS ONE* 7 (7), e40709.
- Jacob, S., Finsterbusch, J., Weishaupt, J.H., Khorram-Sefat, D., Frahm, J., Ehrenreich, H., 2003. Diffusion tensor imaging for long-term follow-up of corticospinal tract degeneration in amyotrophic lateral sclerosis. *Neuroradiology* 45 (9), 598–600.
- Kassubek, J., Unrath, A., Huppertz, H.-J., Lulé, D., Ethofer, T., Sperfeld, A.-D., Ludolph, A.C., 2005. Global brain atrophy and corticospinal tract alterations in ALS, as investigated by voxel-based morphometry of 3-D MRI. *Amyotroph. Lateral Scler. Other Motor Neuron Disord.* 6 (4), 213–220.
- Leemans A, Jeurissen B, Sijbers J, Jones D, editors. ExploreDTI: A graphical toolbox for processing, analyzing, and visualizing diffusion MR data. *Proceedings of the 17th Scientific Meeting, International Society for Magnetic Resonance in Medicine; 2009; Honolulu.*
- Lillo, P., Mioshi, E., Burrell, J.R., Kiernan, M.C., Hodges, J.R., Hornberger, M., Stamatakis, E.A., 2012. Grey and white matter changes across the amyotrophic lateral sclerosis-frontotemporal dementia continuum. *PLoS One* 7 (8), e43993.
- Lulé, D.E., Aho-Özhan, H.E.A., Vázquez, C., Weiland, U., Weishaupt, J.H., Otto, M., Anderl-Straub, S., Semler, E., Uttner, I., Ludolph, A.C., 2019. Story of the ALS-FTD continuum retold: rather two distinct entities. *J. Neurol. Neurosurg. Psychiatry*. 90 (5), 586–589.
- Matte, G.P., Pioro, E.P., 2010. Clinical features and natural history in ALS patients with upper motor neuron abnormalities on conventional brain MRI. *Neurology*. 74 (Suppl 2), A216.
- Mezzapesa, D.M., Ceccarelli, A., Dicuonzo, F., Carella, A., De Caro, M.F., Lopez, M., et al., 2007. Whole-brain and regional brain atrophy in amyotrophic lateral sclerosis. *AJNR Am. J. Neuroradiol.* 28 (2), 255–259.
- Mitsumoto, H., Chad, D.A., Pioro, E.P., 1998. *Amyotrophic Lateral Sclerosis*. F.A. Davis Company, Philadelphia.
- Neary, D., Snowden, J.S., Gustafson, L., Passant, U., Stuss, D., Black, S., Freedman, M., Kertesz, A., Robert, P.H., Albert, M., Boone, K., Miller, B.L., Cummings, J., Benson, D.F., 1998. Frontotemporal lobar degeneration: a consensus on clinical diagnostic criteria. *Neurology*. 51 (6), 1546–1554.
- Neumann, M., Sampathu, D.M., Kwong, L.K., Truax, A.C., Micsenyi, M.C., Chou, T.T., Bruce, J., Schuck, T., Grossman, M., Clark, C.M., McCluskey, L.F., Miller, B.L., Masliah, E., Mackenzie, I.R., Feldman, H., Feiden, W., Kretschmar, H.A., Trojanowski, J.Q., Lee, V.-Y., 2006. Ubiquitinated TDP-43 in frontotemporal lobar degeneration and amyotrophic lateral sclerosis. *Science* 314 (5796), 130–133.
- Omer, T., Finegan, E., Hutchinson, S., Doherty, M., Vajda, A., McLaughlin, R.L., Pender, N., Hardiman, O., Bede, P., 2017. Neuroimaging patterns along the ALS-FTD spectrum: a multiparametric imaging study. *Amyotroph. Lateral Scler. Frontotemporal Degener.* 18 (7-8), 611–623.
- Rajagopalan, V., Liu, Z., Allexandre, D., Zhang, L., Wang, X.-F., Pioro, E.P., Yue, G.H., Le, W., 2013. Brain white matter shape changes in amyotrophic lateral sclerosis (ALS): a fractal dimension study. *PLoS ONE* 8 (9), e73614.
- Rajagopalan, V., Pioro, E.P., 2014. Distinct patterns of cortical atrophy in ALS patients with or without dementia: An MRI VBM study. *Amyotroph. Lateral Scler. Frontotemporal Degener.* 15 (3-4), 216–225.
- Rajagopalan, V., Pioro, E.P., 2017. Differential involvement of corticospinal tract fibers in ALS phenotypes: A diffusion tensor tractography and imaging study. *Neuroimage Clin.* 14, 574–579.
- Rajagopalan, V., Yue, G.H., Pioro, E.P., 2013. Brain white matter diffusion tensor metrics from clinical 1.5T MRI distinguish between ALS phenotypes. *J. Neurol.* 260 (10), 2532–2540.
- Rascovsky, K., Hodges, J.R., Knopman, D., Mendez, M.F., Kramer, J.H., Neuhaus, J., et al., 2011. Sensitivity of revised diagnostic criteria for the behavioural variant of frontotemporal dementia. *Brain*. 134 (Pt 9), 2456–2477.
- Rubinov, M., Sporns, O., 2010. Complex network measures of brain connectivity: uses and interpretations. *NeuroImage*. 52 (3), 1059–1069.
- Sach, M., Winkler, G., Glauche, V., Liepert, J., Heimbach, B., Koch, M.A., et al., 2004. Diffusion tensor MRI of early upper motor neuron involvement in amyotrophic lateral sclerosis. *Brain*. 127 (Pt 2), 340–350.
- Sage, C.A., Peeters, R.R., Gerner, A., Robberecht, W., Sunaert, S., 2007. Quantitative diffusion tensor imaging in amyotrophic lateral sclerosis. *Neuroimage*. 34 (2), 486–499.
- Schimrigk, S.K., Bellenberg, B., Schluter, M., Stieltjes, B., Drescher, R., Rexilius, J., et al., 2007. Diffusion tensor imaging-based fractional anisotropy quantification in the corticospinal tract of patients with amyotrophic lateral sclerosis using a probabilistic mixture model. *AJNR Am. J. Neuroradiol.* 28 (4), 724–730.
- Strong, M.J., 2001. The Evidence for ALS as a Multisystems Disorder of Limited Phenotypic Expression *Canadian Journal of Neurological Sciences*. 28:285-98.
- Tang, M., Chen, X., Zhou, Q., Liu, B., Liu, Y., Liu, S., et al., 2015. Quantitative assessment of amyotrophic lateral sclerosis with diffusion tensor imaging in 3.0T magnetic resonance. *Int. J. Clin. Exp. Med.* 8 (5), 8295–8303.
- Turner, M.R., Hammers, A., Allsop, J., Al-chalabi, A., Shaw, C.E., Brooks, D.J., Nigel Leigh, P., Andersen, P.M., 2007. Volumetric cortical loss in sporadic and familial amyotrophic lateral sclerosis. *Amyotroph. Lateral Scler.* 8 (6), 343–347.
- Tzourio-Mazoyer, N., Landeau, B., Papathanassiou, D., Crivello, F., Etard, O., Delcroix, N., Mazoyer, B., Joliot, M., 2002. Automated anatomical labeling of activations in SPM using a macroscopic anatomical parcellation of the MNI MRI single-subject brain. *NeuroImage*. 15 (1), 273–289.
- Verstraete, E., Veldink, J.H., Mandl, R.C.W., van den Berg, L.H., van den Heuvel, M.P., He, Y., 2011. Impaired structural motor connectome in amyotrophic lateral sclerosis. *PLoS ONE* 6 (9), e24239.